

引用格式：衣可心，Marc Jolivet，郭召杰，2025. 阿尔金断裂带东西两端构造转换与扩展过程：从三联点谈起[J]. 地质力学学报，31(1)：24–38. DOI: [10.12090/j.issn.1006-6616.2024068](https://doi.org/10.12090/j.issn.1006-6616.2024068)

Citation: YI K X, JOLIVET M, GUO Z J, 2025. Tectonic transition and extension at the eastern and western ends of the Altyn Tagh fault: insights from triple junctions[J]. Journal of Geomechanics, 31(1)：24–38. DOI: [10.12090/j.issn.1006-6616.2024068](https://doi.org/10.12090/j.issn.1006-6616.2024068)

阿尔金断裂带东西两端构造转换与扩展过程：从三联点谈起

衣可心^{1,2}，Marc Jolivet²，郭召杰¹

YI Kexin^{1,2}，JOLIVET Marc²，GUO Zhaojie¹

1. 北京大学地球与空间科学学院造山带与地壳演化教育部重点实验室，北京 100871；

2. Géosciences Rennes–UMR CNRS 6118, Université de Rennes, Rennes 35700, France

1. Key Laboratory of Orogenic Belts and Crustal Evolution, School of Earth and Space Sciences, Peking University, Beijing 100871, China;

2. Géosciences Rennes–UMR CNRS 6118, Université de Rennes, Rennes 35700, France

Tectonic transition and extension at the eastern and western ends of the Altyn Tagh fault: insights from triple junctions

Abstract: [Objective] The Altyn Tagh fault (ATF) is the largest left-lateral strike-slip fault on the northern margin of the Qinghai-Tibet Plateau, extending for about 1600 km. It accommodates a considerable portion of the India-Eurasia convergence and is widely regarded as a key tectonic boundary influencing the plateau's uplift and outward growth. However, its mode of propagation remains debated. Resolving this debate requires clarifying how the ATF evolved into its present configuration and how it connects with adjacent structures such as the Qilian orogenic belt and the Qimantagh-Eastern Kunlun fault. In this study, we use the concept of triple junctions to investigate key transition zones at the eastern and western ends of the ATF—namely, the Subei and Tula triple junctions—to shed light on the fault's Cenozoic segmented rupture and bidirectional extension. [Methods] Triple junction analysis, a fundamental method in plate tectonics, is utilized to assess fault properties and fault stability from a kinematic perspective. Additionally, GPS data and seismic source mechanism solutions are analyzed to characterize the current kinematic behaviors and movement directions of the faults. [Results] (1) Transition between ATF and Qilian orogenic belt: Subei triple junction. The central segment of the ATF was the earliest to become active during the Cenozoic, generating a compressional horsetail splay on its eastern termination. The Danghe Nanshan fault and Yemahe-Daxueshan fault emerged as part of this horsetail splay. As left-lateral strike-slip motion on the ATF accelerated in the Miocene, large offsets developed between the Tarim, Qaidam, and Qilian blocks, giving rise to a triple junction near Subei. Initially, this triple junction was unstable, and the Qilian block experienced extensional strain relative to the Tarim block, indicating a local stretching environment. To achieve stability, the ATF progressively “straightened” eastward, ultimately supplanting the Yemahe-Daxueshan fault. Its western segment was reoriented to run parallel to the ATF, while the Danghe Nanshan fault remained as the key boundary on the Qilian side. Consequently, a stable triple junction formed at the intersection of the ATF's central and eastern segments with the Danghe Nanshan fault. At the present leading edge of the ATF's eastward propagation, the Hongliuxia fault displays a similar evolutionary trajectory, suggesting that the ATF continues to extend by reconfiguring secondary faults. (2) Transition between ATF and Qimantagh-Eastern Kunlun fault: Tula triple junction. The ATF's central segment spawned a tensional horsetail splay at its western termination, involving the Tula and Baiganhu faults. When large-scale activity on the Eastern Kunlun fault commenced in the Miocene, the Qaidam block began moving relative to the Eastern Kunlun block, producing

基金项目：国家自然科学基金重点项目（41930213）

This research is financially supported by Key Program of the National Natural Science Foundation of China (Grant No. 41930213).

第一作者：衣可心（1998—），女，在读博士，构造地质学。Email: yikexin@pku.edu.cn

通信作者：郭召杰（1963—），男，博士，教授，构造地质学。Email: zjguo@pku.edu.cn

收稿日期：2024-06-12；修回日期：2024-09-09；录用日期：2024-09-19；网络出版日期：2024-12-13；责任编辑：范二平

an unstable triple junction in the Tula region. To achieve a stable configuration, the ATF propagated westward along a more linear path, gradually diminishing activity on the Baiganhu fault. As a result, the stable triple junction—involving the Tarim, Qaidam, and Eastern Kunlun blocks—ultimately localized where the ATF meets the Qimantagh-Eastern Kunlun fault. This westward “straightening” and the concurrent reduction in subsidiary fault activity have fashioned the current tectonic framework at the western end of the ATF. [Conclusion] (1) The ATF has undergone a segmented rupture–bidirectional extension process throughout the Cenozoic. (2) The Miocene activation of the Yemahe-Daxueshan, the Qimantagh-Eastern Kunlun and other fault systems led to the formation of two triple junctions at Subei and Tula, respectively. These junctions were initially unstable, prompting secondary faults to “shortcut” and realign and leading the ATF to straighten and extend farther east and west. [Significance] This study refines our understanding of how the Altyn Tagh fault expanded along the northern margin of the Qinghai-Tibet Plateau. By applying triple junction concepts to continental blocks, we illustrate how block interactions have governed the ATF’s segmentation and through-going evolution. The proposed segmented rupture–bidirectional extension framework reconciles geological observations of Cenozoic deformation along the ATF. It also underscores the importance of analyzing triple junctions in understanding large-scale tectonic reorganization.

Keywords: Altyn Tagh fault; northern Qinghai-Tibet Plateau; triple junction; tectonic transition; Qilian orogenic belt

摘要: 阿尔金断裂带作为青藏高原北缘的关键构造边界, 其演化历史和构造转换机制对理解青藏高原的生长极为重要。阿尔金断裂带不同分段的构造环境与演化历程不同, 其各自与祁连山造山带和祁曼塔格-东昆仑断裂带的构造转换研究也仍有不足之处。三联点分析是板块构造学中的重要分析方法, 速度三角形反映了断裂属性, 三联点稳定性则从运动学角度揭示了断裂的演化方向和历程。综合地质、地貌与地震资料, 系统分析了阿尔金断裂带中段与东西段代表性的肃北与吐拉三联点的构造特征与活动历史; 并借助三联点稳定性准则, 构建了这 2 个三联点的演化模型。研究结果表明, 野马河-大雪山断裂与祁曼塔格-东昆仑断裂带启动, 不稳定三联点形成并向稳定三联点转化, 促使阿尔金断裂带“截弯取直”, 并在此基础上提出了分段破裂-双向扩展模型。这一结果为理解青藏高原北缘复杂的构造演化历史提供了新的视角。

关键词: 阿尔金断裂带; 青藏高原北缘; 三联点; 构造转换; 祁连山造山带

中图分类号: P542 **文献标识码:** A **文章编号:** 1006-6616(2025)01-0024-15

DOI: 10.12090/j.issn.1006-6616.2024068

0 引言

阿尔金断裂带(Altyn Tagh fault)是青藏高原北缘一条岩石圈尺度的大型左旋走滑边界断裂, 总体呈北东东—南西西向, 是青藏高原最重要的边界断层之一。新生代阿尔金断裂带的构造活动受控于印度-欧亚板块碰撞的远程效应, 多数研究者认为其走滑位移量约为 360 ± 70 km (Peltzer and Tapponnier, 1988; 许志琴等, 1999; Meng et al., 2001; Sobel et al., 2001; Yue et al., 2001; Liu et al., 2007; Cheng et al., 2015a), 吸收了印度与欧亚大陆之间 20%~30% 的缩短量 (Avouac and Tapponnier, 1993; Li et al., 2002; Clark, 2012; Cheng et al., 2015b)。

阿尔金断裂带的扩展生长方式是青藏高原北缘最为重要的科学问题之一, 也是理解青藏高原隆升生长的关键。目前, 研究者针对青藏高原演化提出 3 个主要端元模型, 不同模型均要求阿尔金断裂

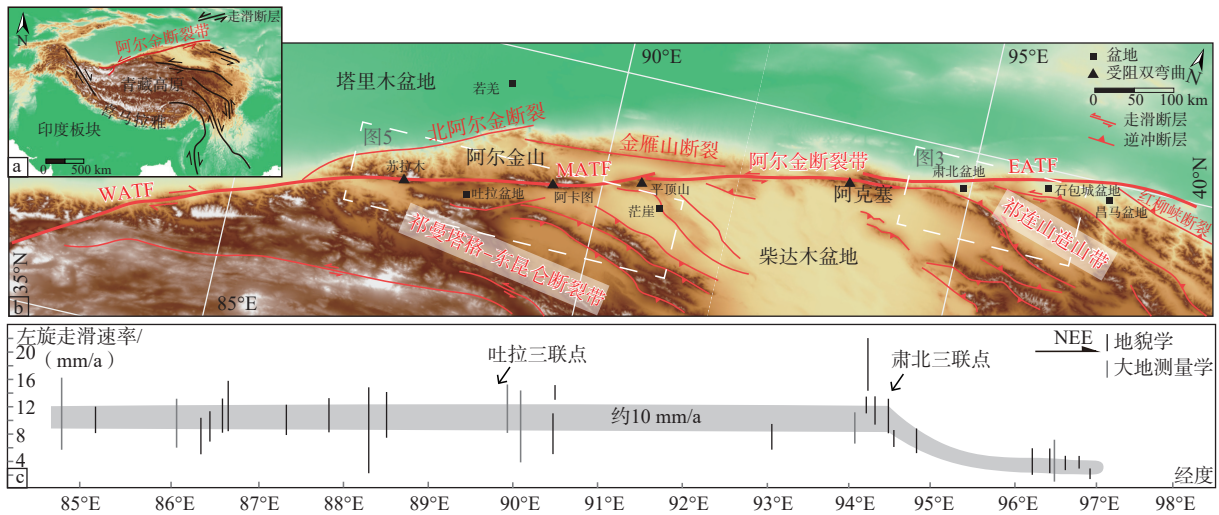
带有与之相适应的不同生长过程: 刚性块体模型强调青藏高原内的块体拼贴增生与挤出, 支持阿尔金断裂带自西向东逐步扩展 (Tapponnier et al., 1982, 2001); 黏性薄席模型支持高原作为整体缩短增厚, 认为阿尔金断裂带应该在印度-欧亚板块碰撞之初快速贯通 (England and McKenzie, 1982; Molnar et al., 1993); 非均质岩石圈模型则强调高原内部岩石圈强弱有别, 不同时期、不同地区的变形主导机制不同, 此种模型下阿尔金断裂带的活动会更为复杂 (Ding et al., 2022)。因此, 阿尔金断裂带在新生代何时开始活动、如何演化到现今的状态, 是限定高原北缘生长模型的重要边界条件。阿尔金断裂带空间差异性巨大, 被多个受阻双弯曲分隔, 与周缘断裂带有复杂的构造转换。阿尔金断裂带分别与祁连山造山带和祁曼塔格-东昆仑断裂带形成的三联点, 是断裂分段演化的断点, 更是构造转换的承载点。文章基于三联点概念, 以阿尔金断裂带东段的

肃北三联点与西段的吐拉三联点为例, 聚焦阿尔金山断裂带不同分段与周缘断裂带的构造转换, 恢复阿尔金山断裂带在新生代分段破裂-贯通的演化过程。

1 阿尔金山断裂带基本特征

阿尔金山断裂带长达 1600 km, 自西向东分隔了塔里木盆地与东昆仑山、柴达木盆地和祁连山, 基于此可大致分为西段(昆仑山段)、中段(柴达木盆地)与东段(祁连山段)。由于昆仑山、祁连山与柴达木盆地岩石圈强度和性质不同(Wang, 2001; 孙

玉军等, 2013; 宋晓东等, 2015; 裴旭等, 2022), 不同分段的演化也相应有所不同。同时, 中段包括平直的主断面和阿尔金山北部的北阿尔金山断裂与金雁山断裂, 发育平顶山双弯曲(约 90.4°E)、阿克塞双弯曲(约 93.7°E)等多个受阻双弯曲(图 1)。而受阻双弯曲等复杂的障碍和其构造几何位置控制着断裂的起始、扩展和终止, 现今仍未完全贯通的平顶山弯曲说明阿尔金山断裂带中段的演化也并非全段整体破裂, 其内部以弯曲为界亦有分段。因此, 分段演化应该是阿尔金山断裂带现今活动研究与构造历史恢复的重要研究思路。



a—青藏高原主要走滑断裂分布图; b—阿尔金山断裂带受阻双弯曲、三联点与邻区主要断裂的位置关系分布图(WATF、MATF、EATF 分别代指阿尔金山断裂带西段、中段与东段); c—阿尔金山断裂带地貌学与大地测量学研究获得的左旋走滑速率分布图(修改自 Wu et al., 2019b)

图 1 阿尔金山断裂带构造简图

Fig. 1 Simplified tectonic map of the Altyn Tagh fault (ATF)

(a) Distribution of major strike-slip faults on the Qinghai-Tibet Plateau; (b) Extension of the ATF and its spatial relationships with neighboring major faults; the double bending, triple junctions, and the positions of the western, central, and eastern segments of the Altyn Tagh fault (WATF, MATF, and EATF, respectively) are shown; (c) Distribution of left-lateral strike-slip rates obtained from geomorphological and geodetic studies of the Altyn Tagh fault (modified from Wu et al., 2019b)

阿尔金山断裂带的不同分段与祁连山造山带和祁曼塔格-东昆仑断裂带共同构成了大型三联点, 通过三联点与周缘断裂带的构造转换是其从分段演化到贯通的关键步骤。现今阿尔金山断裂带与祁连山造山带的构造转换最受关注。大地测量学和构造地貌学研究发现, 阿尔金山断裂带中段的走滑速率约为 10 mm/a, 在阿克塞-肃北以东, 速率快速下降到约 7 mm/a, 并在东端仅为 1~2 mm/a(Zhang et al., 2007; Elliott et al., 2008; Li et al., 2018; 图 1)。徐锡伟等(2003)提出这一变化是三联点附近构造转换的结果, 减少量转换为三联点派生出的祁连山内逆断层

的隆升和走滑。这一观点与经典向东侧向挤出模型吻合(Tapponnier et al., 1982; Meyer et al., 1998), 并得到越来越多构造地貌学、古地震学和大地测量学研究的支持(Xu et al., 2021; Li et al., 2022; Yan et al., 2024)。

相比第四纪构造活动研究, 新生代演化历史中阿尔金山断裂带-祁连山造山带构造转换的研究则相对不足, 作为转换核心的三联点的活动则更加缺乏运动学机制的研究。Cheng et al.(2015b)提出祁连山地壳的新生代缩短量不足以吸收阿尔金山断裂带约 360±40 km 的总走滑量, 强调通过走滑运动祁连山

向东挤出是实现阿尔金断裂带构造转换的重要方式。Yang et al. (2023) 通过解析苏干湖地区的地表和地下构造, 提出新生代早期党河南山的挤压缩短与增厚完全吸收了阿尔金断裂带的走滑量; 中新世以来, 祁连山内走滑断裂系统大规模启动, 块体向东挤出与地壳缩短是阿尔金断裂带-祁连山造山带构造转换的主要形式。这些研究强调祁连山内部的走滑运动, 但并未从运动学机制上深入探讨这些活动对阿尔金断裂带东段演化的影响。

由于野外条件和地质数据的限制, 以往研究鲜少涉及阿尔金断裂带西段与祁曼塔格-东昆仑断裂带的构造转换, 三联点也从未被清晰界定。Cheng et al. (2014) 提出祁曼塔格断裂的分支是东昆仑断裂带西端在阿尔金断裂带作用下逐渐向北迁移的结果, 即祁曼塔格-东昆仑断裂带与阿尔金断裂带的交汇位置(三联点)是不断移动的。

2 三联点概念与应用

三联点(Triple Junction)概念是板块构造理论的重要基石之一, 在 3 个岩石圈板块边界的交汇点即三联点处, 相邻 3 个板块的相对运动速度矢量和为零。三联点概念最早由 Mckenzie and Morgan (1969) 提出, 后经多位学者完善 (York, 1973; Patriat and Courtillot, 1984)。研究者依据板块边界类型洋脊(R)、海沟(T)和转换断层(F), 将三联点分为 RRR、RRT、FFF 等 16 种理论可能, 但现实中出现的三联点类型有限(王振山和魏东平, 2018)。同时, 三联点可分为稳定三联点与不稳定三联点: 前者位置和几何特征不会随板块运动而改变; 相反, 不稳定三联点无法长期存在, 会通过转变断裂的性质、位置和几何特征, 快速转化为不同类型的稳定三联点 (Ingersoll, 1982), 这也是现今只能看到少数几种稳定三联点的原因。

通过 3 个板块边界的类型、方位以及相对运动速度可以分析三联点的稳定条件。用速度矢量代表每个板块的运动, 这 3 个矢量的矢量和为零, 形成闭合的三角形。一般来说, 三联点的稳定性可以通过在速度矢量三角形中作辅助线来判定, 辅助线代表板块交界处(断层)的方位, 代表三联点可以移动的范围。当 3 条辅助线交于一点时, 三联点达到稳定状态, 否则不稳定。对于对称扩张的洋脊(R), 辅助线为三角形中速度线的中垂线; 对于转换断层

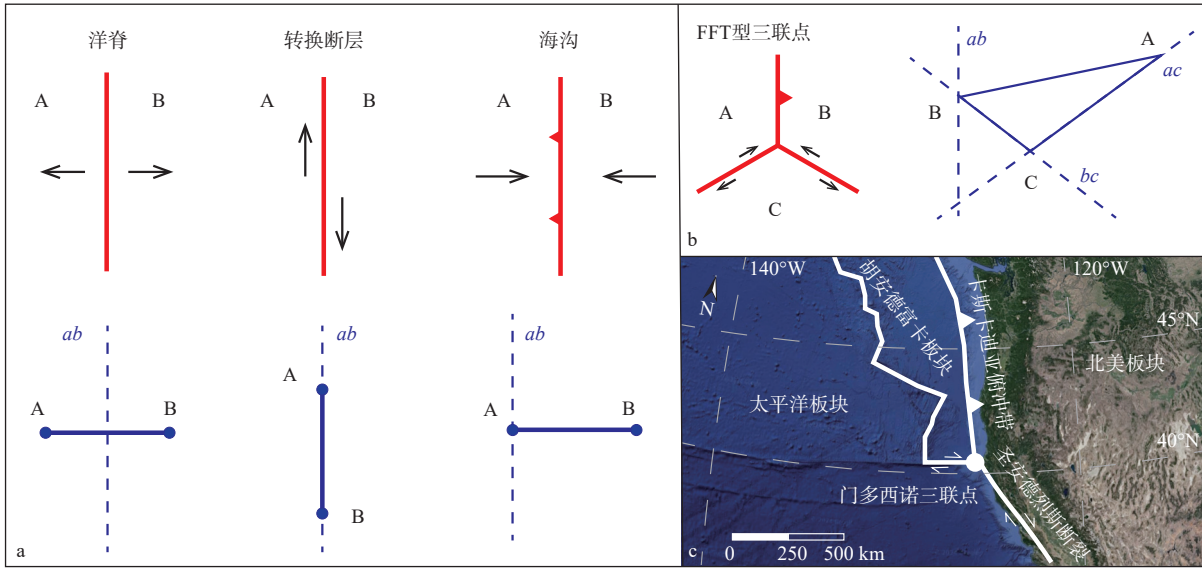
(F), 辅助线为速度的延长线; 对于海沟(T), 辅助线则需过逆冲断层上盘端点, 作海沟的平行线, 此时三联点不会因为俯冲而消亡(图 2a、2b)。

三联点概念对分析断裂之间的相互作用、断裂的演化及对地质地貌具有重要意义。位于北美板块、太平洋板块和胡安德富卡(Juan De Fuca)板块之间的美国西部的门多西诺(Mendocino)三联点(图 2c)稳定性研究是经典实例之一 (Dickinson and Snyder, 1979; Ingersoll, 1982)。作为一个 FFT 型三联点, 门多西诺三联点的稳定条件需要 2 条边界断裂共线(图 2b)。然而, 由于卡斯卡迪亚俯冲带和圣安德烈斯断裂并没有完全共线, 门多西诺三联点并未达到稳定, 而是持续沿圣安德烈斯断裂向北移动, 三联点留下的“岩石圈空隙”导致了周边沉积盆地的沉降、火山喷发和环形地幔流 (Levander et al., 1998; Furlong and Schwartz, 2004; Zandt and Humphreys, 2008)。时至今日, 门多西诺三联点迁移对加州岩石圈、地震和地貌的影响依然备受研究者关注 (Clubb et al., 2020; Shobe et al., 2021; Yeck et al., 2023)。

随着板块构造理论的发展, 三联点概念也被广泛地用于陆内构造块体间的运动学分析, 板块边界类型的洋脊、转换断层和海沟, 可以分别对应块体间的正断层、走滑断层和逆断层(田勤俭和丁国瑜, 1998; Steigerwald et al., 2020), 但对应条件需要进一步厘定。一般来说, 相对刚性的岩石块体的整体运动可以类比到板块运动, 可以借鉴三联点概念分析, 岩石圈块体边界属性可以类比不同的板块边界, 而造山带或者盆地内部的构造转换不宜使用三联点分析。

青藏高原东北缘的三联点研究最早可以追溯到田勤俭和丁国瑜(1998)对海原附近青藏块体、鄂尔多斯地块和阿拉善块体形成的三联点的运动和构造特征分析。徐锡伟等(2003)利用地貌学识别了阿尔金断裂带东段肃北、石包城、疏勒河等多个三联点, 并强调了左旋走滑与垂直活动之间的构造转换关系, 完善了高原北缘的运动学模型。实际上, 在造山带或者陆内一般断裂带相交位置构造运动学的转变, 并非都是三联点的转换, 三联点关注的核心是块体边界断层的相互影响。

青藏高原北缘的主要构造单位之间有较大的性质差异: ①塔里木盆地和柴达木盆地均为巨厚中新世沉积盆地, 地球物理研究揭示了二者基底都是典型的刚性克拉通块体, 相较周缘山脉具有低温



A、B、C代表不同的板块；红色实线代表板块边界，蓝色虚线 ab 、 bc 、 ac 则代表板块AB、板块BC和板块AC之间的边界辅助线； ab 、 bc 共线或者 ac 、 bc 共线时稳定

a—三联点稳定性辅助线作法示意图；b—以FFT型三联点为例，说明三联点速度三角形及辅助线的作法，修改自McKenzie and Morgan (1969)；c—Mendocino三联点(FFT型)(Ingersoll, 1982)

图2 三联点原理示意图

Fig. 2 Schematic diagram of triple junction principles

(a) Schematic diagram illustrating the method of constructing auxiliary lines for triple junction stability; (b) An FFT-type triple junction is used as an example for the construction of the triple junction velocity triangle and auxiliary lines, adapted from McKenzie and Morgan (1969); (c) Mendocino triple junction (FFT-type) (Ingersoll, 1982)

In (a) and (b), A, B, and C represent different tectonic plates; the red solid lines denote plate boundaries, while the blue dashed lines ab , bc , and ac represent auxiliary boundary lines between Plate AB, Plate BC, and Plate AC, respectively. The triple junction is stable when ab and bc are collinear or when ac and bc are collinear.

热结构和更高的岩石圈强度(Wang, 2001; 孙玉军等, 2013; 宋晓东等, 2015); 东昆仑山和祁连山同为青藏高原内部大型造山带, 均为古生代—中生代造山带重新活化而成, 且现今依然活跃(Law and Allen, 2020)。②大地电磁研究显示, 阿尔金断裂带形成巨大的电磁各向异性异常, 而祁连山内部的异常较小(Dong et al., 2024); 东昆仑山岩石圈强度大, 形成高电阻屏障(Yu et al., 2020)。③大地测量学研究也指出青藏高原北缘地区的水平应变集中于阿尔金断裂带主断裂沿线(Liu et al., 2024), 祁连地块和东昆仑地块内部相对稳定, 且具有旋转等刚性块体特征。因此, 文中在讨论青藏高原北缘的构造运动中主要关注塔里木地块、柴达木地块、祁连地块和东昆仑地块之间的相对运动, 当然不可否认的是其内部也都发育明显的变形, 但与块体间的运动相比可能不在一个数量级, 因此可以简化借用三联点概念进行分析。

文中所使用的地震数据下载自 Global CMT

(www.globalcmt.org; Dziewonski et al., 1981; Ekström et al., 2012), 在Python软件中通过PyGMT绘制震源机制解(Tian et al., 2024)。原始GPS数据来自Wang and Shen(2020)与Ge et al.(2022), 并使用FORTRAN语言将GPS数据从ITRF2014旋转至塔里木参考系, 获得研究区域相对塔里木盆地的运动速度, 并使用PyGMT绘制成图(Tian et al., 2024)。

3 阿尔金断裂带与祁连山造山带构造转换：以肃北三联点为例

3.1 断裂特征与活动历史

祁连山造山带由一系列北西走向的断裂组成, 自南向北包括党河南山断裂、野马河—大雪山断裂和昌马断裂等多条大型断裂。这些断裂向西止于阿尔金断裂带, 与阿尔金断裂带形成了多个交点。文章以阿尔金断裂带与南祁连山党河南山断裂西段形成的肃北三联点为例, 探究阿尔金断裂带东段

构造转换的特点。

肃北三联点可视为塔里木地块、祁连地块和柴达木地块的交汇处, 现在由阿尔金断裂带中段、东段和党河南山断裂组成(图 3)。野马河-大雪山断

裂的西段也汇入肃北地区, 具有复杂的几何构造: 西段为北东东向, 与阿尔金断裂带平行; 中段沿大雪山向东延伸; 东段为北西向, 与党河南山断裂平行。

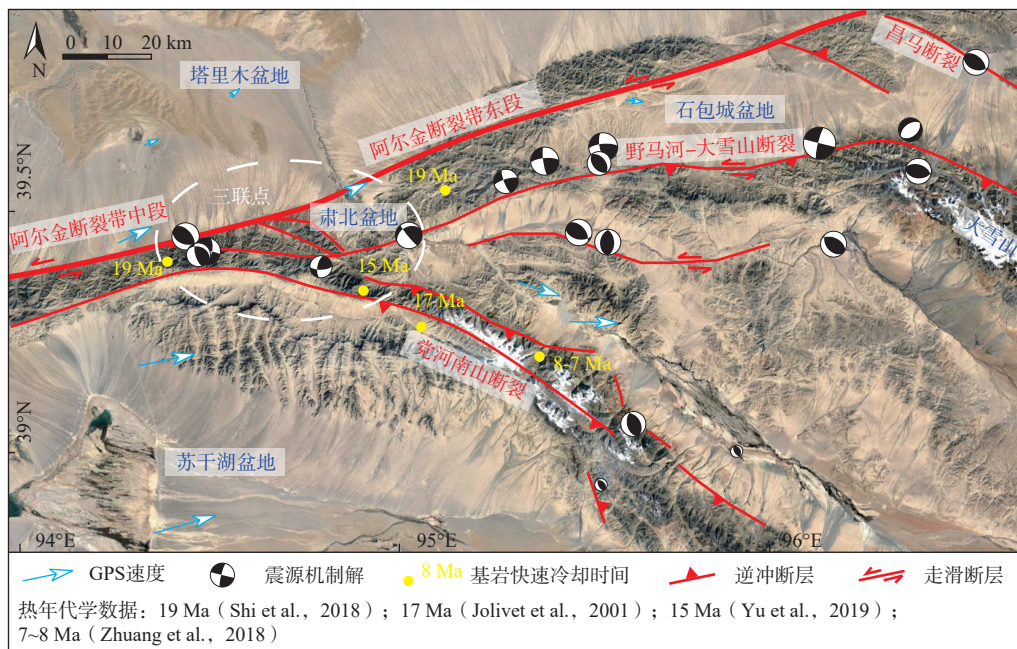


图 3 肃北三联点及周边区域构造简图

Fig. 3 Tectonic map of the Subei triple junction and the surrounding area

肃北盆地的沉积序列记录了三联点区域最早的构造活动。研究者曾对西水沟、铁匠沟等剖面进行了磁性地层学、沉积学和低温年代学研究, 认为该地区的渐新世泥岩 (Yin et al., 2002) 或中新世晚期的砾岩 (Wang et al., 2003; Sun et al., 2005; Lin et al., 2015; Lu et al., 2022) 指示了初始构造变形与抬升。低温年代学研究提出党河南山在古新世至渐新世就已经隆升并剥露 (Li et al., 2017; He et al., 2020), 在中新世构造抬升更为显著 (Shi et al., 2018; Yu et al., 2019), 并持续活动至今 (Yi et al., 2022; 图 3)。

相比之下, 由于野外交通条件的限制, 阿尔金断裂带东段和野马河-大雪山断裂的启动时间研究不足。Jolivet et al. (2001) 曾对野马河与阿尔金断裂带间山脉的热年代学定年获得其冷却年龄约为 19 Ma。冯志硕等 (2010) 通过剖析石包城盆地疏勒河组的岩石沉积特征, 发现该盆地沉积颗粒呈东南粗、西北细的特征, 古流向证据进一步指示其物源来自大雪山; 而现今西北部的阿尔金断裂带东段沿线并未发育边缘相的粗碎屑沉积物, 而是发育沉积中心相的细粒层系。据此推测, 野马河-大雪山断裂在中新世活动增强, 大雪山快速隆升, 石包城盆

地整体呈东南高、西北低的构造背景; 之后阿尔金断裂带东段启动, 在走滑拉分作用下形成了现今的石包城盆地。

党河南山断裂现今的构造属性和运动速度依然存在争议。该断裂第四纪逆冲活动强烈, 发育大量断层陡坎, 其活动特征已被深入研究 (Shao et al., 2017; 罗浩等, 2020)。Xu et al. (2021) 通过对错断的河流阶地进行宇宙成因核素 ^{10}Be 定年, 提出党河南山断裂的抬升速率约为 $0.6 \pm 0.2 \text{ mm/a}$ 。与此同时, 党河南山断裂是否具有走滑运动分量或走滑属性始终存在分歧。Meyer et al. (1998) 基于震源机制解结果, 提出党河南山断裂具有左旋走滑分量。但由于 GPS 数据受到台站分布的影响, 目前尚没有足够清晰的数据表征其走滑运动方向特征 (图 3; Xu et al., 2021)。因此, 文章暂时将党河南山断裂作为逆断层进行分析, 即使其具有走滑分量也不影响相关运动学分析。

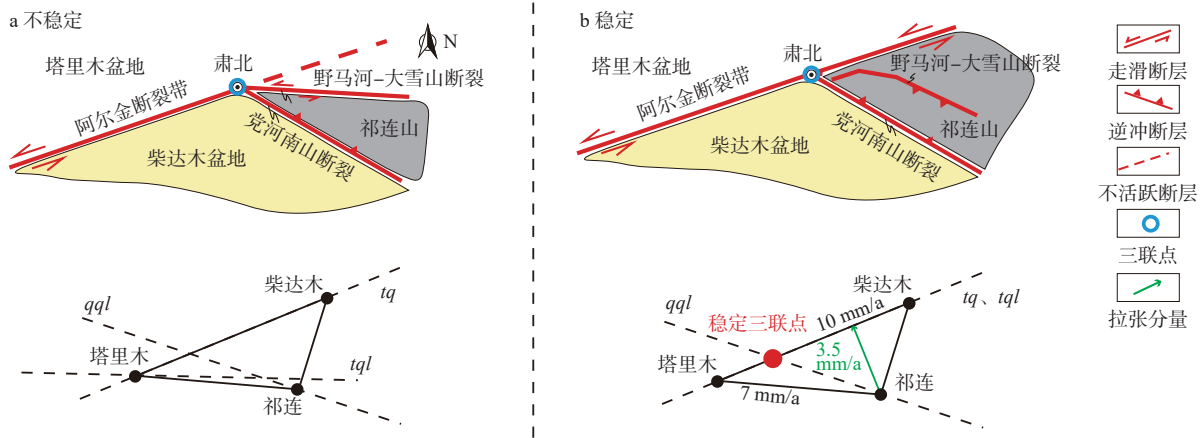
震源机制解显示, 野马河-大雪山断裂西段以左旋走滑为主, 兼具逆冲分量 (图 3)。通过实测地貌面错动数据和热释光定年, 估算该断裂的平均水平滑动速率为 $1.27 \pm 0.18 \text{ mm/a}$, 平均逆冲速率为

0.4 ± 0.07 mm/a。Luo et al. (2015) 基于更为精细的地貌测量和年代学分析, 提出野马河-大雪山断裂水平滑动速率约为 2.18 ± 0.32 mm/a、逆冲速率为 0.4 ± 0.07 mm/a。相比阿尔金断裂带在肃北以西约 10 mm/a、肃北以东约 7 mm/a 的走滑速率, 野马河-大雪山断裂的滑动速率较小, 且不同分段走向、性质有所区别, 说明其可能经历了多期复杂的构造演化。

3.2 三联点运动学分析与演化

在肃北三联点, 将构造活动简化为塔里木地

块、柴达木地块和祁连地块这 3 个地块之间的相对运动(图 4)。按上文断裂发育时限分析, 阿尔金断裂带中段和党河南山断裂最晚在渐新世已有活动, 且阿尔金断裂带东段的活动晚于野马河-大雪山断裂。因此, 推测阿尔金断裂带中段最早活动, 在尾部形成挤压型马尾扇, 组成马尾扇的断裂即为党河南山断裂与野马河-大雪山断裂的雏形。由于此时变形发生在祁连块体内部而非块体之间, 因此不适用三联点分析。



速度矢量三角形中 tq 、 tml 、 qql 分别代表塔里木地块与柴达木地块、塔里木地块与祁连地块、柴达木地块与祁连地块的辅助线

图 4 肃北三联点稳定性演化示意图

Fig. 4 Diagram of the stability evolution of the Subei triple junction

In the velocity vector triangle, tq , tml , and qql represent auxiliary lines connecting the Tarim and Qaidam blocks, the Tarim and Qilian blocks, and the Qaidam and Qilian blocks, respectively.

随着中新世阿尔金断裂带走滑运动的加速, 显著增加的大位移量造成不同单元块体间的大规模相对位移, 党河南山断裂与野马河-大雪山断裂成为分隔 3 个块体间明显相对运动的边界, 在肃北附近形成三联点。此时三联点的组成为: 阿尔金断裂带中段为左旋走滑断裂(F), 党河南山为逆冲断裂(T), 野马河-大雪山断裂西段以左旋走滑为主(F), 肃北三联点可以被视为 FFT 型的三联点。由于地质体走滑速率的计算往往是依据地质体在一定地质历史时期内的位移获得的平均速度, 难以分段测量, 而且结果争议较大。因此文章借鉴现今 GPS 监测得到的断裂运动速率, 将其作为阿尔金断裂带不同分段中新世的运动速率。阿尔金断裂带中段的走滑速率为 10 mm/a, 即塔里木地块与柴达木地块的相对速度; 阿尔金断裂带东段的走滑速率取 7 mm/a, 即塔里木地块与祁连地块相对速度在阿尔金断裂带方向上的分量为 7 mm/a (Zhang et al., 2007)。根据速度矢量三角形可知, 除阿尔金断裂带东段的走滑分

量外, 祁连地块相对于塔里木地块有垂直于阿尔金断裂带的拉张分量, 约为 3.5 mm/a, 即两者间存在伸展环境。这一伸展环境即是祁连造山带最西端发育石包城盆地、昌马盆地而非挤压隆升高山的构造条件。

由三联点分析可知, 只要党河南山断裂和野马河-大雪山断裂不平行, 边界辅助线 tml (塔里木与祁连地块)、 qql (柴达木与祁连地块) 与 tq (塔里木与柴达木地块) 就没有交点, 即阿尔金断裂带中段、党河南山断裂与野马河-大雪山断裂这 3 条断裂无法形成稳定的三联点(图 4), 这种情况不会长期存在。为了转化成稳定三联点, 阿尔金断裂带向东直线延伸, 野马河-大雪山断裂被逐渐置换替代, 其西段被改造至与阿尔金断裂带平行。阿尔金断裂带的中段、东段与党河南山断裂形成了稳定的三联点。值得注意的是, 尽管分析中使用现今速度数据对中新世三联点进行分析, 但速度大小变化仅影响速度矢量三角形的相对形状, 稳定性判断主要取决于 3 条边界的方向位置, 与速度大小无关, 因此该三联点

稳定性分析不受相对运动速度的具体数值影响。

在现今阿尔金断裂带扩展的最前缘, 红柳峡断裂并不与阿尔金断裂带主断裂平行, 而是呈约 20° 的夹角, 与当时野马河-大雪山断裂极为相似。因此可以推测, 随着阿尔金断裂带运移量的不断累积, 阿尔金断裂带、红柳峡断裂与北祁连山断裂组成的三联点会经历与当初肃北三联点相似的构造演化, 并最终促使阿尔金断裂带继续沿直线扩展。

4 阿尔金断裂带与祁曼塔格-东昆仑断裂带构造转换: 以吐拉三联点为例

4.1 断裂特征与活动历史

祁曼塔格-东昆仑断裂带是位于柴达木盆地与

东昆仑地块之间的大型左旋走滑断裂系, 主体为东西向展布, 西端在祁曼塔格地区形成一系列北西西向的线性断裂, 并组成弓形构造。这些线性断裂与阿尔金断裂带在吐拉盆地处相交, 因此, 文章将由塔里木地块、柴达木地块和东昆仑地块交汇区域简化成三联点, 称为吐拉三联点(图 5)。

吐拉三联点处北东向的断裂包括阿尔金断裂带西段、中段, 吐拉断裂与白干湖断裂。阿尔金断裂带基本平直, 走滑速率约为 $9\sim 10\text{ mm/a}$ (He et al., 2013); 白干湖断裂位于吐拉盆地与祁曼塔格山脉之间, 发育线性构造地貌, 东北段隐伏并可能延伸至阿尔金山中, 表明其最新活动并不明显, 断裂为左旋走滑断裂。

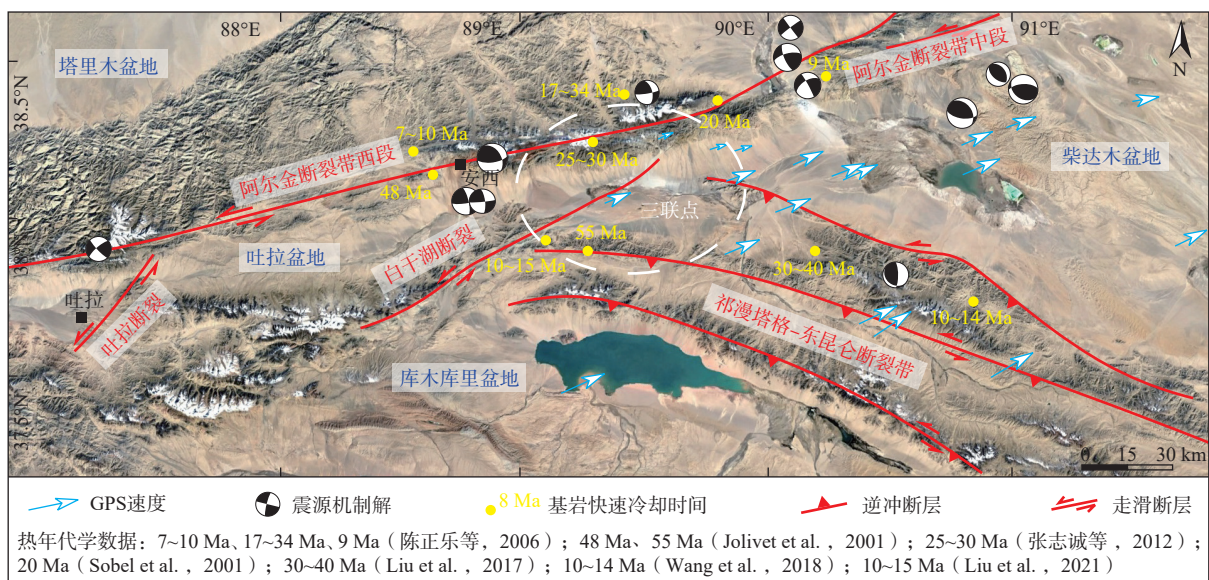


图 5 吐拉三联点及周边区域构造简图

Fig. 5 Tectonic map of the Tula triple junction and surrounding area

阿尔金断裂带西段沿线的热年代学研究揭示了其始新世与中新世的活动, 而吐拉断裂与白干湖断裂的活动历史则更为复杂。相关学者通过对比吐拉剖面、安西煤矿附近剖面与柴达木盆地采石岭剖面的岩性、化石发育特征以及碎屑锆石组成指示的源区特征等证据, 发现其发育相似的侏罗系、古新统和始新统地层特征, 提出吐拉盆地和柴达木盆地因为阿尔金断裂带的早期活动而分离(郭召杰和张志诚, 1998; Cheng et al., 2015a)。据此推断, 此时作为吐拉盆地边界的吐拉断裂与白干湖断裂在中新世及之前为阿尔金断裂带的分支断裂。Liu et al.(2021)基于白干湖断裂的地貌学与低温热年代学

研究, 提出白干湖断裂是与阿尔金断裂带密切相关且相连的走滑断裂, 在中新世存在强烈的活动。结合已有研究和现今的地貌特征, 推测现今吐拉盆地的边界——吐拉断裂与白干湖断裂, 在新生代早期为阿尔金断裂带的尾端分支断裂, 在中新世发生大规模走滑运动, 逐渐分离了吐拉盆地与柴达木盆地。

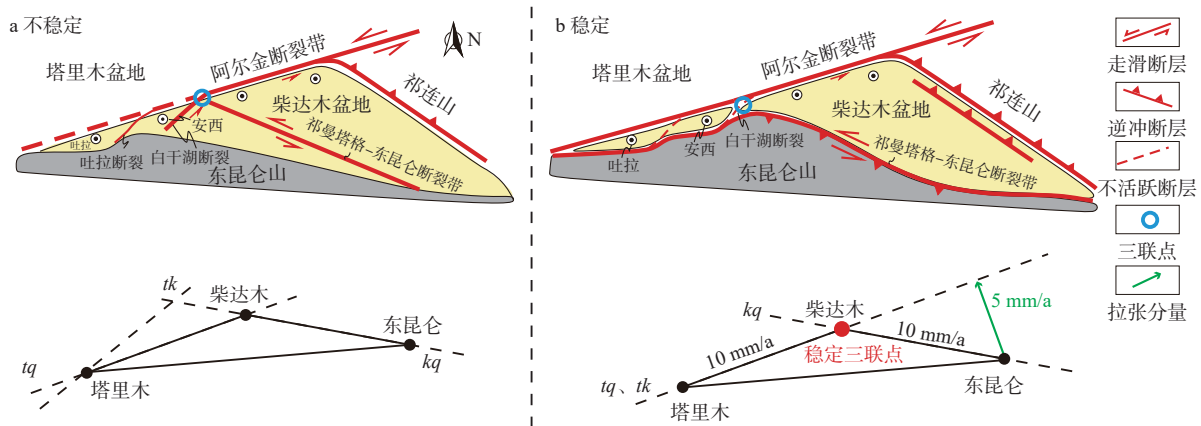
三联点处北西向的断裂为祁曼塔格-东昆仑断裂带。研究普遍认为, 东昆仑断裂带在中新世启动, 并伴随着东昆仑山的大规模隆升(Duvall et al., 2013; Wu et al., 2019a, 2021)。Cheng et al.(2014)基于祁曼塔格山北缘断裂的地震剖面和地貌特征提出,

东昆仑断裂带西端受阿尔金断裂带左旋走滑位移的影响,自中新世以来自南向北逐渐迁移,形成近平行的祁曼塔格断裂带。在此模型中,祁曼塔格断裂带是东昆仑断裂带尾端移动的记录。

东昆仑断裂带的左旋走滑运动缺乏定量制约,根据现今大地测量学和地貌学估计其走滑速率约为 10 mm/a,向东逐渐降低至 2 mm/a(Kirby et al., 2007; Harkins et al., 2010; Li et al., 2011)。震源机制解和台站相对塔里木盆地的 GPS 数据显示,现今祁曼塔格断裂带以逆冲运动为主,兼具左旋走滑分量(图 5; Ge et al., 2022),而断裂的滑动速率则缺乏数据。由于祁曼塔格断裂带与东昆仑断裂带性质相似、成因相同,在后续讨论中,文章将两者简化为祁曼塔格-东昆仑断裂带。

4.2 三联点运动学分析与演化

在吐拉段,将构造活动简化为塔里木地块、柴达木地块和东昆仑地块之间相对运动(图 6),塔里木-柴达木地块与柴达木-东昆仑地块间的边界速度取自阿尔金断裂带西段和祁曼塔格-东昆仑断裂带的走滑速率,均约为 10 mm/a。由速度矢量三角形可知,东昆仑地块相对于塔里木地块的速度可以分解为沿阿尔金断裂带的左旋走滑分量和垂直阿尔金断裂带约为 5 mm/a 的拉张分量。因此,阿尔金断裂带西段以左旋走滑为主,且处于伸展环境。这一特征仍体现在现今的阿尔金断裂带西端,例如在伸展背景下发育的阿什库勒盆地。此外,该地区的地震活动以拉张型强震为主(Bie and Ryder, 2014; Pan et al., 2015),并伴随活跃的火山活动(李海兵等, 2006)。



速度矢量三角形中 tq 、 tk 、 kq 分别代表塔里木地块与柴达木地块、塔里木地块与东昆仑地块、东昆仑地块与塔里木地块的辅助线

图 6 吐拉三联点稳定性演化示意图

Fig. 6 Diagram of the stability evolution of the Tula triple junction

In the velocity vector triangle, tq , tk , and kq represent auxiliary lines connecting the Tarim and Qaidam blocks, the Tarim and Eastern Kunlun blocks, and the Eastern Kunlun and Qaidam blocks, respectively.

结合白干湖断裂的几何特征,推测该三联点的运动演化过程为:阿尔金断裂带初始活动时以中段的运动为主,西部尾端派生的吐拉断裂与白干湖断裂组成伸展型马尾扇构造,此时变形局限于昆仑地块内部,3个块体间尚没有大规模相对位移,没有形成三联点。在东昆仑断裂中新世的大规模活动开始后,柴达木地块和东昆仑地块相对运动,形成了三联点,而此时3条边界辅助线不能相交于一点,即无法形成稳定三联点。为了达到稳定状态,阿尔金断裂带沿直线向西延伸,白干湖断裂的活动逐渐减弱。此时,边界辅助线 tq (塔里木地块与柴达木地块)和 tk (塔里木地块与东昆仑地块)重合,三联点在阿尔金断裂带与祁曼塔格-东昆仑断裂带的交

点处达到稳定,形成了现今的构造格局。

值得注意的是,由于柴达木地块伴随着阿尔金断裂带的走滑活动向北移动,祁曼塔格地区的断裂会向北迁移,形成发散状的断裂带,而且具有逆冲分量。所以吐拉三联点无法如肃北三联点一样集中,而是在一定区域内移动,没有明确固定的位置。这与以往对祁曼塔格-昆北断裂带的研究相一致(Cheng et al., 2014, 2015c)。

5 讨论

5.1 阿尔金断裂带东西两端构造转换方式

阿尔金断裂带、祁连山造山带和祁曼塔格-东

昆仑断裂带是青藏高原北部最为重要的 3 条大型构造带, 三者的活动与相互影响控制着高原北缘的几何特征和构造框架。三联点作为大型块体边界断裂带的交汇点, 是协调青藏高原不同块体间相互运动和构造变形的关键节点。肃北三联点和吐拉三联点的构造特征反应了阿尔金断裂带东、西两端构造转换的方式与差异。

在阿尔金断裂带东段, 祁连山边缘与内部多个逆冲和走滑断裂共同吸收了阿尔金断裂带的左旋位移, 表现为块体的抬升与挤出; 在阿尔金断裂带西段, 祁曼塔格-东昆仑断裂带共同通过大型左旋走滑运动吸收印度板块的运动量。地震统计数据表明, 肃北三联点主要断裂沿线均有地震记录, 吐拉三联点的地震活动则集中在阿尔金断裂带的双弯曲处, 说明前者的构造运动更为活跃, 三联点构造转换更加集中。从阿尔金断裂带的滑动速率测量中可知, 在肃北三联点的东、西两侧, 阿尔金断裂带的走滑速率明显下降; 相反, 在吐拉三联点附近, 阿尔金断裂带的活动速率没有明显变化, 而三联点位置也随着祁曼塔格-东昆仑断裂带的移动在一定范围内迁移。在地貌活动上, 党河南山和大雪山断裂前缘均发育冲断带, 且在第四纪以来具有持续加强的趋势 (Xu et al., 2021; Yi et al., 2022); 祁曼塔格断裂与白干湖断裂的构造地貌发育则更为成熟, 仅有小规模错断的河流显示较弱的断裂活动 (Liu et al., 2021), 体现断裂活动仅局限于块体内部。

阿尔金断裂带东、西两端不同构造转换方式的差异反应了阿尔金断裂带和青藏高原演化的方向性和阶段性。随着青藏高原的向北、向外扩展, 祁连山造山带的活动不断增强, 并至今仍在向北逆冲; 相反, 祁曼塔格-东昆仑断裂带的活动主要受制于青藏高原的挤出, 以东部的走滑断裂为主, 逆冲活动相对较弱。因此, 吐拉三联点记录了始新世-中新世阿尔金断裂带和祁曼塔格-东昆仑断裂带的活动; 肃北三联点则反映了青藏高原北缘从早期响应碰撞到后期大幅隆升的全过程。

5.2 三联点演化对阿尔金断裂带扩展的意义

阿尔金断裂带长达 1600 km, 其扩展生长方式一直备受争议, 具有代表性的观点包括北向扩展、快速贯通、双向扩展和构造重组 4 个模型。北向扩展模型依托于经典的青藏高原北向生长模型, 认为阿尔金断裂带随青藏高原向东北方向扩展 (Métivier et al., 1998; Meyer et al., 1998; Tapponnier et al., 2001;

Wang et al., 2006, 2016)。快速贯通模型基于低温年代学和沉积记录, 认为阿尔金断裂带在新生代早期便作为大型走滑断裂带, 快速贯通至祁连山, 随后在断裂系统内部逐渐演化形成现今面貌 (Yin et al., 2002)。这一假设更符合强调同步变形的黏性薄席高原模型。阿尔金断裂带在这两个经典模型之外, 近年来学者依据更丰富的研究资料提出了更复杂的扩展模型, 如双向扩展模型依据低温年代学数据分布、沉积速率的变化和古地磁偏角的研究, 认为断裂从中段向东、西两端双向扩展, 且强调中新世以来阿尔金断裂带构造活动在不断加强 (Li et al., 2021; 谢皓等, 2022); 构造重组模型依托近年来对北阿尔金山的研究成果, 提出阿尔金断裂带的走滑运动最初由北阿尔金断裂承担, 并与金雁山形成大型的受阻弯曲, 现今的主断裂在中新世才开始贯通活动 (Wu et al., 2019b; Gao et al., 2022)。

虽然这些模型都能解释所在区域的构造现象, 但结论扩展到阿尔金断裂带全段时, 会出现矛盾或者难以解释之处。最重要的是, 阿尔金断裂带中段和北段存在大量新生代早期走滑断裂的证据, 北向扩展模型和构造重组模型难以解释。近期 Yi et al. (2024) 通过对同构造沉积中的碳酸盐岩 U-Pb 定年, 证实 59 Ma 阿尔金断裂带的走滑活动在现今索尔库里盆地启动, 即阿尔金断裂带中段最早破裂; 肃北盆地始新世的快速沉积也与阿尔金断裂带构造活动有关 (宋春晖, 2006); 吐拉盆地与柴达木盆地的分离也需要早期阿尔金断裂带的走滑活动 (Cheng et al., 2015a)。相比之下, 快速贯通模型和双向扩展模型能解释绝大多数沉积和热年代学记录, 但扩展的过程和机制讨论仍需完善。

在此基础上, 文章提出分段破裂-双向扩展的模型: 柴达木段的阿尔金断裂带最先启动, 反映了阿尔金断裂带活动的本质——塔里木与柴达木 2 个大型刚性块体间的走滑运动。同时, 断裂两端派生出了次级构造, 在东端形成挤压型马尾扇, 导致新生代早期党河南山西端的隆升与肃北盆地内沉积记录; 在西段形成拉张型马尾扇, 表现为吐拉盆地内沉积及其与柴达木盆地的初始分离 (图 7a)。中新世时期, 由于青藏高原活动增强, 阿尔金断裂带变形量增加, 现有的断裂难以吸收全部的位移, 造成多块体间规模较大的相对位移, 在阿尔金断裂带两端形成三联点 (图 7b)。鉴于三联点稳定性的要求, 阿尔金断裂带“截弯取直”, 原本的马尾断裂

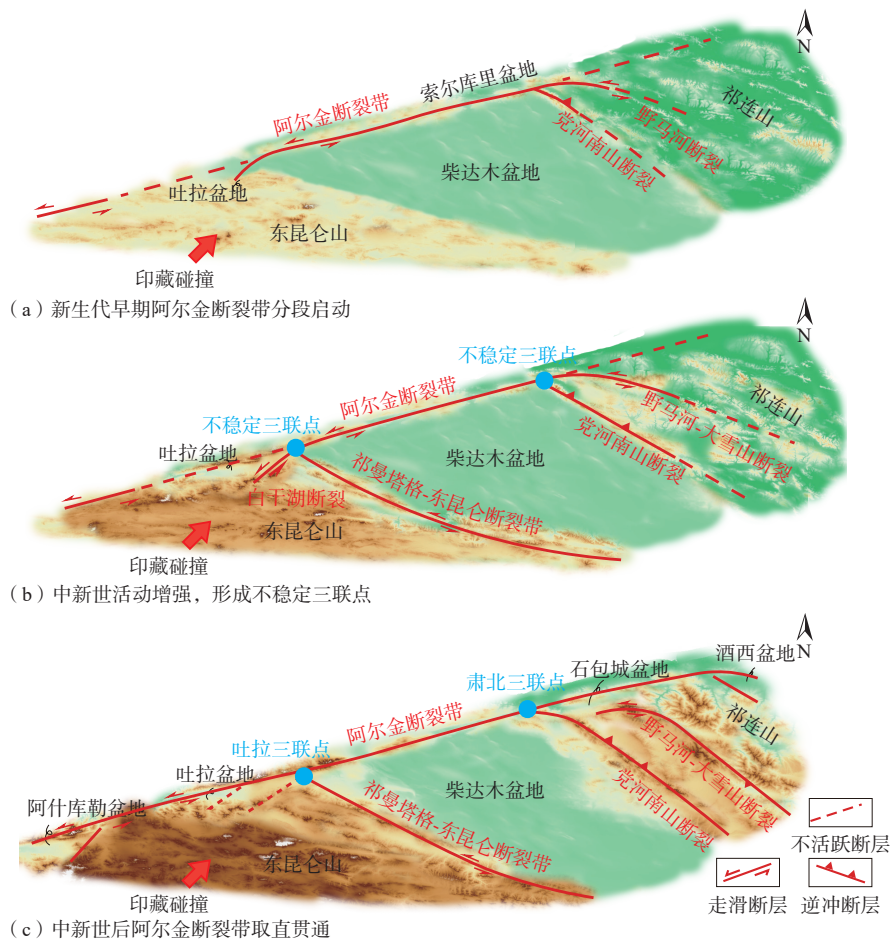


图7 阿尔金断裂带与三联点演化示意图

Fig. 7 Diagram of the evolution of the Altyn Tagh fault and triple junctions

(a) Early Cenozoic segmental initiation of the Altyn Tagh Fault (ATF); (b) Miocene activity enhancement, leading to the formation of unstable triple junctions; (c) Post-Miocene shortcutting and through-going of the ATF.

被废弃,主断裂沿直线向东西两端扩展,与此前可能的分段断裂相贯通,组成现今长达1600 km的大型断裂(图7c)。

阿尔金断裂带这一双向扩展的演化过程,响应了青藏高原同步启动、变形向北扩展的特征,突出了柴达木盆地、祁连山和东昆仑山不同岩石圈特征对断裂演化的影响,支持了非均质岩石圈模型。青藏高原内断裂广布,大型断裂之间的构造转换复杂,构成了多个三联点,三联点概念和分析应用具有更大的推广空间。

6 结论

- (1) 阿尔金断裂带在新生代经历了分段破裂-双向扩展的演化历程。
- (2) 中新世野马河-大雪山断裂与祁曼塔格-东

昆仑断裂带的启动导致不稳定的肃北三联点和吐拉三联点形成,促使阿尔金断裂带“截弯取直”,向东西两端扩展。类似的扩展在现今的阿尔金断裂带两端持续进行,这是阿尔金断裂带扩展的主要方式。

(3) 三联点特征分析对揭示板块/地块交界处的运动学关系、分析断裂之间的相互作用与断裂属性具有重要意义,在区域构造分析中有广泛应用价值。**致谢:**感谢加州大学洛杉矶分校沈正康教授分享GPS数据与FORTRAN代码、并给予帮助。杨屹洲博士参与了最初讨论,在此表示感谢。

References

- AVOUAC J P, TAPPONNIER P, 1993. Kinematic model of active deformation in Central Asia[J]. *Geophysical Research Letters*, 20(10): 895-898.
- BIE L D, RYDER I, 2014. Recent seismic and aseismic activity in the Ashikule stepover zone, NW Tibet[J]. *Geophysical Journal International*, 198(3): 1632-1643.

- CHEN Z L, GONG H L, LI L, et al., 2006. Cenozoic uplifting and exhumation process of the Altyn Tagh mountains[J]. *Earth Science Frontiers*, 13(4): 91-102. (in Chinese with English abstract)
- CHENG F, JOLIVET M, FU S T, et al., 2014. Northward growth of the Qimen Tagh Range: a new model accounting for the Late Neogene strike-slip deformation of the SW Qaidam Basin[J]. *Tectonophysics*, 632: 32-47.
- CHENG F, GUO Z J, JENKINS H S, et al., 2015a. Initial rupture and displacement on the Altyn Tagh fault, northern Tibetan Plateau: constraints based on residual Mesozoic to Cenozoic strata in the western Qaidam Basin[J]. *Geosphere*, 11(3): 921-942.
- CHENG F, JOLIVET M, DUPONT-NIVET G, et al., 2015b. Lateral extrusion along the Altyn Tagh Fault, Qilian Shan (NE Tibet): insight from a 3D crustal budget[J]. *Terra Nova*, 27(6): 416-425.
- CHENG X, FU S T, WANG H F, et al., 2015c. Geometry and kinematics of the Arlar strike-slip fault, SW Qaidam basin, China: new insights from 3-D seismic data[J]. *Journal of Asian Earth Sciences*, 98: 198-208.
- CLARK M K, 2012. Continental collision slowing due to viscous mantle lithosphere rather than topography[J]. *Nature*, 483(7387): 74-77.
- CLUBB F J, MUDD S M, HURST M D, et al., 2020. Differences in channel and hillslope geometry record a migrating uplift wave at the Mendocino triple junction, California, USA[J]. *Geology*, 48(2): 184-188.
- DICKINSON W R, SNYDER W S, 1979. Geometry of triple junctions related to San Andreas Transform[J]. *Journal of Geophysical Research: Solid Earth*, 84(B2): 561-572.
- DING L, KAPP P, CAI F L, et al., 2022. Timing and mechanisms of Tibetan Plateau uplift[J]. *Nature Reviews Earth & Environment*, 3(10): 652-667.
- DONG Z Y, XIAO Q B, SUN Z L, et al., 2024. Crustal electrical anisotropic structure of the Altyn Tagh fault in the Subei Area, NW China: implications for fault zone architecture[J]. *Journal of Geophysical Research: Solid Earth*, 129(7): e2023JB028550.
- DUVALL A R, CLARK M K, KIRBY E, et al., 2013. Low-temperature thermochronometry along the Kunlun and Haiyuan Faults, NE Tibetan Plateau: Evidence for kinematic change during late-stage orogenesis[J]. *Tectonics*, 32(5): 1190-1211.
- DZIEWONSKI A M, CHOU T A, WOODHOUSE J H, 1981. Determination of earthquake source parameters from waveform data for studies of global and regional seismicity[J]. *Journal of Geophysical Research: Solid Earth*, 86(B4): 2825-2852.
- EKSTRÖM G, NETTLES M, DZIEWOŃSKI A M, 2012. The global CMT project 2004-2010: Centroid-moment tensors for 13, 017 earthquakes[J]. *Physics of the Earth and Planetary Interiors*, 200-201: 1-9.
- ELLIOTT J R, BIGGS J, PARSONS B, et al., 2008. InSAR slip rate determination on the Altyn Tagh Fault, northern Tibet, in the presence of topographically correlated atmospheric delays[J]. *Geophysical Research Letters*, 35(12): L12309.
- ENGLAND P, MCKENZIE D, 1982. A thin viscous sheet model for continental deformation[J]. *Geophysical Journal International*, 70(2): 295-321.
- FENG Z S, ZHANG Z C, LI J F, et al., 2010. Study on Cenozoic sedimentary characteristics and its relationship with the Altyn Tagh Fault in Shibaodan Basin, Gansu[J]. *Chinese Journal of Geology*, 45(1): 181-193. (in Chinese with English abstract)
- FURLONG K P, SCHWARTZ S Y, 2004. Influence of the Mendocino triple junction on the tectonics of coastal California[J]. *Annual Review of Earth and Planetary Sciences*, 32: 403-433.
- GAO S B, COWGILL E, WU L, et al., 2022. From left slip to transpression: Cenozoic tectonic evolution of the North Altyn Fault, NW margin of the Tibetan Plateau[J]. *Tectonics*, 41(3): e2021TC006962.
- GE W P, SHEN Z K, MOLNAR P, et al., 2022. GPS determined asymmetric deformation across central Altyn Tagh fault reveals rheological structure of Northern Tibet[J]. *Journal of Geophysical Research: Solid Earth*, 127(9): e2022JB024216.
- GUO Z J, ZHANG Z C, 1998. Structural style and tectonic evolution of the basins in the Altun Region[J]. *Geological Review*, 44(4): 357-364. (in Chinese with English abstract)
- HARKINS N, KIRBY E, SHI X, et al., 2010. Millennial slip rates along the eastern Kunlun fault: implications for the dynamics of intracontinental deformation in Asia[J]. *Lithosphere*, 2(4): 247-266.
- HE J K, VERNANT P, CHÉRY J, et al., 2013. Nailing down the slip rate of the Altyn Tagh fault[J]. *Geophysical Research Letters*, 40(20): 5382-5386.
- HE P J, SONG C H, WANG Y D, et al., 2020. Early Cenozoic exhumation in the Qilian Shan, northeastern margin of the Tibetan Plateau: insights from detrital apatite fission track thermochronology[J]. *Terra Nova*, 32(6): 415-424.
- INGERSOLL R V, 1982. Triple-junction instability as cause for late Cenozoic extension and fragmentation of the western United States[J]. *Geology*, 10(12): 621-624.
- JOLIVET M, BRUNEL M, SEWARD D, et al., 2001. Mesozoic and Cenozoic tectonics of the northern edge of the Tibetan Plateau: fission-track constraints[J]. *Tectonophysics*, 343(1-2): 111-134.
- KIRBY E, HARKINS N, WANG E Q, et al., 2007. Slip rate gradients along the eastern Kunlun fault[J]. *Tectonics*, 26(2): TC2010.
- LAW R, ALLEN M B, 2020. Diachronous Tibetan Plateau landscape evolution derived from lava field geomorphology[J]. *Geology*, 48(3): 263-267.
- LEVANDER A, HENSTOCK T J, MELTZER A S, et al., 1998. Fluids in the lower crust following Mendocino triple junction migration: active basaltic intrusion?[J]. *Geology*, 26(2): 171-174.
- LI A, LIU R, ZHANG S M, et al., 2022. Evidence of structural transformation in the eastern part of the Altyn Tagh Fault, northern margin of the Tibetan Plateau, China, based on the kinematics and shortening rate of the Hongliuxia region[J]. *Journal of Asian Earth Sciences*, 240: 105445.
- LI B S, YAN M D, ZHANG W L, et al., 2021. Bidirectional growth of the Altyn Tagh Fault since the Early Oligocene[J]. *Tectonophysics*, 815: 228991.
- LI C X, XU X W, WEN X Z, et al., 2011. Rupture segmentation and slip partitioning of the mid-eastern part of the Kunlun Fault, north Tibetan Plateau[J]. *Science China Earth Sciences*, 54(11): 1730-1745.
- LI H B, YANG J S, SHI R D, et al., 2002. Determination of the Altyn Tagh strike-slip fault basin and its relationship with mountains[J]. *Chinese Science Bulletin*, 47(7): 572-577.
- LI H B, YANG J S, XU Z Q, et al., 2006. The constraint of the Altyn Tagh fault system to the growth and rise of the northern Tibetan plateau[J]. *Earth Science Frontiers*, 13(4): 59-79. (in Chinese with English abstract)

- LI J F, ZHANG Z C, ZHAO Y, et al., 2017. Detrital apatite fission track analyses of the Subei basin: implications for basin-range structure of the northern Tibetan Plateau[J]. *International Geology Review*, 59(2): 204-218.
- LI Y C, SHAN X J, QU C Y, et al., 2018. Crustal deformation of the Altyn Tagh fault based on GPS[J]. *Journal of Geophysical Research: Solid Earth*, 123(11): 10309-10322.
- LIN X, ZHENG D W, SUN J M, et al., 2015. Detrital apatite fission track evidence for provenance change in the Subei Basin and implications for the tectonic uplift of the Danghe Nan Shan (NW China) since the mid-Miocene[J]. *Journal of Asian Earth Sciences*, 111: 302-311.
- LIU C J, JI L Y, ZHU L Y, et al., 2024. Interseismic strain rate distribution model of the Altyn Tagh Fault constrained by InSAR and GPS[J]. *Earth and Planetary Science Letters*, 642: 118884.
- LIU D L, LI H B, SUN Z M, et al., 2017. AFT dating constrains the Cenozoic uplift of the Qimen Tagh Mountains, Northeast Tibetan Plateau, comparison with LA-ICPMS Zircon U-Pb ages[J]. *Gondwana Research*, 41: 438-450.
- LIU D L, LI H B, CHEVALIER M L, et al., 2021. Activity of the Baiganhu Fault of the Altyn Tagh Fault System, northern Tibetan Plateau: insights from zircon and apatite fission track analyses[J]. *Palaeogeography, Palaeoclimatology, Palaeoecology*, 570: 110356.
- LIU Y J, NEUBAUER F, GENSER J, et al., 2007. Geochronology of the initiation and displacement of the Altyn Strike-Slip Fault, western China[J]. *Journal of Asian Earth Sciences*, 29(2-3): 243-252.
- LIU H J, SANG S P, WANG P, et al., 2022. Initial uplift of the Qilian Shan, northern Tibet since ca. 25 Ma: implications for regional tectonics and origin of Eolian deposition in Asia[J]. *GSA Bulletin*, 134(9-10): 2531-2547.
- LUO H, HE W G, YUAN D Y, et al., 2015. Slip Rate of Yema River-Daxue Mountain Fault since the Late Pleistocene and Its Implications on the Deformation of the Northeastern Margin of the Tibetan Plateau[J]. *Acta Geologica Sinica-English Edition*, 89(2): 561-574.
- LUO H, XU X W, LIU X L, et al., 2020. The structural deformation pattern in the eastern segment of the Altyn Tagh fault[J]. *Acta Geologica Sinica*, 94(3): 692-706. (in Chinese with English abstract)
- MCKENZIE D P, MORGAN W J, 1969. Evolution of triple Junctions[J]. *Nature*, 224(5215): 125-133.
- MENG Q R, HU J M, YANG F Z, 2001. Timing and magnitude of displacement on the Altyn Tagh fault: constraints from stratigraphic correlation of adjoining Tarim and Qaidam basins, NW China[J]. *Terra Nova*, 13(2): 86-91.
- MÉTIVIER F, GAUDEMER Y, TAPPONNIER P, et al., 1998. Northeastward growth of the Tibet Plateau deduced from balanced reconstruction of two depositional areas: The Qaidam and Hexi Corridor basins, China[J]. *Tectonics*, 17(6): 823-842.
- MEYER B, TAPPONNIER P, BOURJOT L, et al., 1998. Crustal thickening in Gansu-Qinghai, lithospheric mantle subduction, and oblique, strike-slip controlled growth of the Tibet Plateau[J]. *Geophysical Journal International*, 135(1): 1-47.
- MOLNAR P, ENGLAND P, MARTINOD J, 1993. Mantle dynamics, uplift of the Tibetan Plateau, and the Indian monsoon[J]. *Reviews of Geophysics*, 31(4): 357-396.
- PAN J W, LI H B, VAN DER WOERD J, et al., 2015. The first quantitative slip-rate estimated along the ashikule fault at the western segment of the Altyn Tagh fault system[J]. *Acta Geologica Sinica-English Edition*, 89(6): 2088-2089.
- PATRIAT P, COURTILLOT V, 1984. On the stability of triple junctions and its relation to episodocity in spreading[J]. *Tectonics*, 3(3): 317-332.
- PEI X, HUANGFU P P, LI Z H, et al., 2022. Why Qaidam Basin is amalgamated into Tibetan Plateau but Tarim basin is not?[J]. *Chinese Journal of Geophysics*, 65(11): 4259-4272. (in Chinese with English abstract)
- PELTZER G, TAPPONNIER P, 1988. Formation and evolution of strike-slip faults, rifts, and basins during the India-Asia Collision: an experimental approach[J]. *Journal of Geophysical Research: Solid Earth*, 93(B12): 15085-15117.
- SHAO Y X, YUAN D Y, OSKIN M E, et al., 2017. Historical (Yuan Dynasty) Earthquake on the North Danghe Nanshan Thrust, Western Qilian Shan, China[J]. *Bulletin of the Seismological Society of America*, 107(3): 1175-1184.
- SHI W B, WANG F, YANG L K, et al., 2018. Diachronous growth of the Altyn Tagh mountains: constraints on propagation of the Northern Tibetan margin from (U-Th)/he dating[J]. *Journal of Geophysical Research: Solid Earth*, 123(7): 6000-6018.
- SHOBE C M, BENNETT G L, TUCKER G E, et al., 2021. Boulders as a lithologic control on river and landscape response to tectonic forcing at the Mendocino triple junction[J]. *GSA Bulletin*, 133(3-4): 647-662.
- SOBEL E R, ARNAUD N, JOLIVET M, et al., 2001. Jurassic to Cenozoic exhumation history of the Altyn Tagh range, northwest China, constrained by $^{40}\text{Ar}/^{39}\text{Ar}$ and apatite fission track thermochronology [C]//HENDRIX M S, DAVIS G A. Paleozoic and Mesozoic tectonic evolution of central and Eastern Asia: from continental assembly to intracontinental deformation. Boulder: Geological Society of America.
- SONG C H, 2006. Tectonic uplift and Cenozoic sedimentary evolution in the northern margin of the Tibetan Plateau[D]. Lanzhou: Lanzhou University. (in Chinese with English abstract)
- SONG X D, LI J T, BAO X W, et al., 2015. Deep structure of major basins in Western China and implications for basin formation and evolution[J]. *Earth Science Frontiers*, 22(1): 126-136. (in Chinese with English abstract)
- STEIGERWALD L, EINARSSON P, HJARTARDÓTTIR Á R, 2020. Fault kinematics at the Hengill Triple Junction, SW-Iceland, derived from surface fracture pattern[J]. *Journal of Volcanology and Geothermal Research*, 391: 106439.
- SUN Y J, DONG S W, FAN T Y, et al., 2013. 3D rheological structure of the continental lithosphere beneath China and adjacent regions[J]. *Chinese Journal of Geophysics*, 56(9): 2936-2946. (in Chinese with English abstract)
- SUN Z M, YANG Z Y, PEI J L, et al., 2005. Magnetostratigraphy of Paleogene sediments from northern Qaidam Basin, China: Implications for tectonic uplift and block rotation in northern Tibetan Plateau[J]. *Earth and Planetary Science Letters*, 237(3-4): 635-646.
- TAPPONNIER P, PELTZER G, LE DAIN A Y, et al., 1982. Propagating extension tectonics in Asia: new insights from simple experiments with plas-

- ticine[J]. *Geology*, 10(12): 611-616.
- TAPPONNIER P, ZHIQIN X, ROGER F, et al., 2001. Oblique stepwise rise and growth of the Tibet Plateau[J]. *Science*, 294(5547): 1671-1677.
- TIAN D, UIEDA L, LEONG W J, et al., 2024. PyGMT: A Python interface for the Generic Mapping Tools[J/OL]. Zenodo, 2024-09. Available from: <https://doi.org/10.5281/zenodo.13679420>.
- TIAN Q J, DING G Y, 1998. The tectonic feature of a quasi trijunction in the northeastern corner of Qinghai Xizang Plateau[J]. *Earthquake Research in China*, 14(4): 27-35. (in Chinese with English abstract)
- WANG E, XU F Y, ZHOU J X, et al., 2006. Eastward migration of the Qaidam basin and its implications for Cenozoic evolution of the Altyn Tagh fault and associated river systems[J]. *GSA Bulletin*, 118(3-4): 349-365.
- WANG M, SHEN Z K, 2020. Present-day crustal deformation of continental China derived from GPS and its tectonic implications[J]. *Journal of Geophysical Research: Solid Earth*, 125(2): e2019JB018774.
- WANG W T, ZHANG P Z, PANG J Z, et al., 2016. The Cenozoic growth of the Qilian Shan in the northeastern Tibetan Plateau: a sedimentary archive from the Jiuxi Basin[J]. *Journal of Geophysical Research: Solid Earth*, 121(4): 2235-2257.
- WANG X M, WANG B Y, QIU Z X, et al., 2003. Danghe area (western Gansu, China) biostratigraphy and implications for depositional history and tectonics of northern Tibetan Plateau[J]. *Earth and Planetary Science Letters*, 208(3-4): 253-269.
- WANG Y, 2001. Heat flow pattern and lateral variations of lithosphere strength in China mainland: constraints on active deformation[J]. *Physics of the Earth and Planetary Interiors*, 126(3-4): 121-146.
- WANG Y D, ZHENG J J, ZHENG Y W, 2018. Mesozoic-Cenozoic exhumation history of the Qimen Tagh Range, northeastern margins of the Tibetan Plateau: evidence from apatite fission track analysis[J]. *Gondwana Research*, 58: 16-26.
- WANG Z S, WEI D P, 2018. Research progress on the formation and evolution of triple junctions of global plate motions[J]. *Progress in Geophysics*, 33(5): 1834-1843. (in Chinese with English abstract)
- WU C, ZUZA A V, ZHOU Z G, et al., 2019a. Mesozoic-Cenozoic evolution of the Eastern Kunlun Range, central Tibet, and implications for basin evolution during the Indo-Asian collision[J]. *Lithosphere*, 11(4): 524-550.
- WU C, LI J, DING L, 2021. Low-temperature thermochronology constraints on the evolution of the Eastern Kunlun Range, northern Tibetan Plateau[J]. *Geosphere*, 17(4): 1193-1213.
- WU L, LIN X B, COWGILL E, et al., 2019b. Middle Miocene reorganization of the Altyn Tagh fault system, northern Tibetan Plateau[J]. *GSA Bulletin*, 131(7-8): 1157-1178.
- XIE H, LIU C C, ZHANG H P, et al., 2022. Cenozoic evolution of the Altyn Tagh fault: evidence from sedimentary records of basins along the fault[J]. *Acta Petrologica Sinica*, 38(4): 1107-1125. (in Chinese with English abstract)
- XU Q, HETZEL R, HAMPEL A, et al., 2021. Slip rate of the Danghe Nan Shan thrust fault from ^{10}Be exposure dating of folded river terraces: implications for the strain distribution in Northern Tibet[J]. *Tectonics*, 40(4): e2020TC006584.
- XU X W, TAPPONNIER P, VAN DER WOERD J, et al., 2003. Late Quaternary sinistral slip rate along the Altyn Tagh fault and its structural transformation model[J]. *Science in China (Series D)*, 33(10): 967-974. (in Chinese with English abstract)
- XU Z Q, YANG J S, ZHANG J X, et al., 1999. A comparison between the tectonic units on the two sides of the Altyn Sinistral strike-slip fault and the mechanism of lithospheric shearing[J]. *Acta Geologica Sinica*, 73(3): 193-205. (in Chinese with English abstract)
- YAN B, CHEN P, GAO Y, 2024. Stepwise decrease in strike-slip rate along the eastern Altyn Tagh Fault and its relation to the Qilian Shan thrust system, northeastern Tibetan Plateau[J]. *Journal of Structural Geology*, 179: 105037.
- YANG Y Z, WANG Z D, LIU R C, et al., 2023. Evolution of kinematic transformation from the Altyn Tagh fault to the Qilian Shan in the northern Tibetan Plateau: from early Cenozoic initiation to mid-Miocene extrusion[J]. *Frontiers in Earth Science*, 11: 1250640.
- YECK W L, SHELLY D R, MATERNA K Z, et al., 2023. Dense geophysical observations reveal a triggered, concurrent multi-fault rupture at the Mendocino Triple Junction[J]. *Communications Earth & Environment*, 4(1): 94.
- YI K X, CHENG F, YANG Y Z, et al., 2022. Pleistocene northward thrusting of the Danghe Nanshan: Implications for the growth of the Qilian Shan, Northeastern Tibetan Plateau[J]. *Tectonophysics*, 838: 229476.
- YI K X, CHENG F, JOLIVET M, et al., 2024. Carbonate U-Pb ages constrain Paleocene motion along the Altyn Tagh fault in response to the India-Asia collision[J]. *Geophysical Research Letters*, 51(8): e2023GL107716.
- YIN A, RUMELHART P E, BUTLER R, et al., 2002. Tectonic history of the Altyn Tagh fault system in northern Tibet inferred from Cenozoic sedimentation[J]. *GSA Bulletin*, 114(10): 1257-1295.
- YORK D, 1973. Evolution of Triple Junctions[J]. *Nature*, 244(5415): 341-342.
- YU G, LI M, SHAO G L, et al., 2020. Electrical resistivity variations of lithospheric mantle beneath the northern Tibetan Plateau with tectonic implications[J]. *Journal of Asian Earth Sciences*, 198: 104273.
- YU J X, ZHENG D W, PANG J Z, et al., 2019. Miocene range growth along the Altyn Tagh fault: insights from apatite fission track and (U-Th)/He thermochronometry in the Western Danghenan Shan, China[J]. *Journal of Geophysical Research: Solid Earth*, 124(8): 9433-9453.
- YUE Y J, RITTS B D, GRAHAM S A, 2001. Initiation and long-term slip history of the Altyn Tagh fault[J]. *International Geology Review*, 43(12): 1087-1093.
- ZANDT G, HUMPHREYS E, 2008. Toroidal mantle flow through the western U. S. slab window[J]. *Geology*, 36(4): 295-298.
- ZHANG P Z, MOLNAR P, XU X W, 2007. Late Quaternary and present-day rates of slip along the Altyn Tagh Fault, northern margin of the Tibetan Plateau[J]. *Tectonics*, 26(5): TC5010.
- ZHANG Z C, GUO Z J, LI J F, et al., 2012. Mesozoic and Cenozoic uplift-denudation along the Altyn Tagh fault, Northwestern China: constraints from apatite fission track data[J]. *Quaternary Sciences*, 32(3): 499-509. (in Chinese with English abstract)
- ZHUANG G S, JOHNSTONE S A, HOURIGAN J, et al., 2018. Understand-

ing the geologic evolution of Northern Tibetan Plateau with multiple thermochronometers[J]. *Gondwana Research*, 58: 195-210.

附中文参考文献

- 陈正乐, 宫红良, 李丽, 等, 2006. 阿尔金山脉新生代隆升-剥露过程[J]. *地学前缘*, 13(4): 91-102.
- 冯志硕, 张志诚, 李建锋, 等, 2010. 甘肃石包城盆地新生代沉积特征及与阿尔金断裂的关系研究[J]. *地质科学*, 45(1): 181-193.
- 郭召杰, 张志诚, 1998. 阿尔金盆地群构造类型与演化[J]. *地质论评*, 44(4): 357-364.
- 李海兵, 杨经绥, 许志琴, 等, 2006. 阿尔金断裂带对青藏高原北部生长、隆升的制约[J]. *地学前缘*, 13(4): 59-79.
- 罗浩, 徐锡伟, 刘小利, 等, 2020. 阿尔金断裂东段的构造转换模式[J]. *地质学报*, 94(3): 692-706.
- 裴旭, 皇甫鹏鹏, 李忠海, 等, 2022. 为何塔里木盆地独立于青藏高原整体变形之外而柴达木盆地却并入其中?[J]. *地球物理学报*, 65(11): 4259-4272.
- 宋春晖, 2006. 青藏高原北缘新生代沉积演化与高原构造隆升过程[D]. 兰州: 兰州大学.
- 宋晓东, 李江涛, 鲍学伟, 等, 2015. 中国西部大型盆地的深部结构及对盆地形成和演化的意义[J]. *地学前缘*, 22(1): 126-136.
- 孙玉军, 董树文, 范桃园, 等, 2013. 中国大陆及邻区岩石圈三维流变结构[J]. *地球物理学报*, 56(9): 2936-2946.
- 田勤俭, 丁国瑜, 1998. 青藏高原东北隅似三联点构造特征[J]. *中国地震*, 14(4): 27-35.
- 王振山, 魏东平, 2018. 全球板块运动三联点形成与演化规律的研究进展[J]. *地球物理学进展*, 33(5): 1834-1843.
- 谢皓, 刘彩彩, 张会平, 等, 2022. 新生代阿尔金断裂带的演化: 来自沿线盆地沉积记录的启示[J]. *岩石学报*, 38(4): 1107-1125.
- 徐锡伟, TAPPONNIER P, VAN DER WOERD J, 等, 2003. 阿尔金断裂带晚第四纪左旋走滑速率及其构造运动转换模式讨论[J]. *中国科学(D辑)*, 33(10): 967-974.
- 许志琴, 杨经绥, 张建新, 等, 1999. 阿尔金断裂两侧构造单元的对比及岩石圈剪切机制[J]. *地质学报*, 73(3): 193-205.
- 张志诚, 郭召杰, 李建锋, 等, 2012. 阿尔金断裂带中段中新生代隆升历史分析: 裂变径迹年龄制约[J]. *第四纪研究*, 32(3): 499-509.